

Optical arbitrary waveform characterization via dual-quadrature spectral interferometry

V.R. Supradeepa, Daniel E. Leaird and Andrew M. Weiner

School of Electrical and Computer Engineering, Purdue University, West Lafayette, Indiana 47907, USA.
venkatas@purdue.edu, leaird@purdue.edu, amw@ecn.purdue.edu.

Abstract: We introduce the use of dual-quadrature spectral interferometry for amplitude and phase characterization of 100% duty factor optical arbitrary waveforms generated via spectral line-by-line pulse shaping. We demonstrate this technique for measurement of optical arbitrary waveforms composed of ~30 spectral lines from a 10 GHz frequency comb with 1.4 μ s data acquisition time at an average power level of 10 microwatts. We then demonstrate coherent spectral phase measurements of pulses strongly dispersed by propagation over 50km of optical fiber.

©2008 Optical Society of America

OCIS codes: (320.7100) Ultrafast measurements; (320.5540) Pulse shaping; (320.5520) Pulse compression; (060.2300) Fiber measurements; (120.3940) Metrology

References and links

1. Z. Jiang, D. S. Seo, D. E. Leaird, and A. M. Weiner. "Spectral line by line pulse shaping," *Opt. Lett.* **30**, 1557–1559 (2005).
2. Z. Jiang, C. B. Huang, D. E. Leaird, and A. M. Weiner, "Optical arbitrary waveform processing of more than 100 spectral comb lines," *Nature Photon.* **1**, 463–467 (2007).
3. R. P. Scott, N. K. Fontaine, J. Cao, K. Okamoto, B. H. Kolner, J. P. Heritage, and S. J. B. Yoo, "High-fidelity line-by-line optical waveform generation and complete characterization using FROG," *Opt. Express* **15**, 9977–9988 (2007).
4. D. Miyamoto, K. Mandai, T. Kurokawa, S. Takeda, T. Shioda, and H. Tsuda, "Waveform-Controllable Optical Pulse Generation Using an Optical Pulse Synthesizer," *IEEE Photon. Technol. Lett.* **18**, 721–723 (2006).
5. K. Takiguchi, K. Okamoto, T. Kominato, H. Takahashi, and T. Shibata, "Flexible pulse waveform generation using silica-waveguide-based spectrum synthesis circuit," *Electron. Lett.* **40**, 537–538 (2004).
6. D. J. Kane and R. Trebino, "Characterization of arbitrary femtosecond pulses using frequency-resolved optical gating," *IEEE J. Quantum Electron.* **29**, 571–579 (1993).
7. P. O'Shea, M. Kimmel, X. Gu, and R. Trebino, "Highly simplified device for ultrashort-pulse measurement," *Opt. Lett.* **26**, 932–934 (2001).
8. C. Iaconis and I. A. Walmsley, "Spectral phase interferometry for direct electric-field reconstruction of ultrashort optical pulses," *Opt. Lett.* **23**, 792–794 (1998).
9. L. Lepetit, G. Cheriaux, and M. Joffre, "Linear techniques of phase measurement by femtosecond spectral interferometry for applications in spectroscopy," *J. Opt. Soc. Am. B* **12**, 2467– (1995).
10. E. Frumker, E. Tal, Y. Silberberg, and D. Majer, "Femtosecond pulse-shape modulation at nanosecond rates," *Opt. Lett.* **30**, 2796–2798 (2005).
11. J. T. Willits, A. M. Weiner, and S. T. Cundiff, "Theory of rapid-update line-by-line pulse shaping," *Opt. Express* **16**, 315–327 (2008).
12. Z. Jiang, D. E. Leaird, and A. M. Weiner, "Optical Arbitrary Waveform Generation and Characterization Using Spectral Line-by-Line Control," *J. Lightwave Technol.* **24**, 2487– (2006).
13. R. Trebino, *Frequency resolved optical gating: The measurement of ultrashort optical pulses* (Springer publications, 2002).
14. D. N. Fittinghoff, J. L. Bowie, J. N. Sweetser, R. T. Jennings, M. A. Krumbügel, K. W. DeLong, R. Trebino, and I. A. Walmsley, "Measurement of the intensity and phase of ultraweak, ultrashort laser pulses," *Opt. Lett.* **21**, 884–886 (1996).
15. F. K. Fatemi, T. F. Carruthers, and J. W. Lou, "Characterisation of telecommunications pulse trains by Fourier-transform and dual-quadrature spectral interferometry," *Electron. Lett.* **39**, 921–922 (2003).

16. C. -B. Huang, S. -G. Park, D. E. Leaird, and A. M. Weiner, "Nonlinearly broadened phase-modulated continuous-wave laser frequency combs characterized using DPSK decoding," *Opt. Express* **16**, 2520-2527 (2008).
 17. http://www.andor.com/scientific_cameras/idus-ingaas/models/?iProductCodeID=71.
 18. S. M. Foreman, K. W. Holman, D. D. Hudson, D. J. Jones, and J. Ye, "Remote transfer of ultrastable frequency references via fiber networks," *Rev. Sci. Instrum.* **78**, 021101 (2007).
 19. F. Narbonneau, M. Lours, S. Bize, A. Clairon, G. Santarelli, O. Lopez, Ch. Daussy, A. Amy-Klein, and Ch. Chardonnet, "High resolution frequency standard dissemination via optical fiber metropolitan network," *Rev. Sci. Instrum.* **77**, 064701 (2006).
-

1. Introduction

Interest has recently arisen in optical arbitrary waveform generation (OAWG), in which pulse shaping is used to manipulate optical frequency combs on a line by line basis [1-5]. OAWG leads to new challenges in waveform characterization associated with the unique attributes of fields generated through line by line pulse shaping. In particular, such fields may exhibit 100% duty cycle, with shaped waveforms spanning the full time domain repetition period of the frequency comb, and with spectral amplitude and phase changing abruptly from line to line. Such fields are also characterized by large time-bandwidth product, equal approximately to the number of lines in the shaped frequency comb. Although methods for full characterization of ultrashort pulse fields are well developed, e.g., [6-9], such methods are typically applied to measurement of low duty cycle pulses that are isolated in time, with spectra that are smoothly varying, and with relatively low time-bandwidth product. These properties correspond to low spectral resolution insufficient to capture the rapid spectral changes that are a hallmark of line by line pulse shaping. In general, it is also desirable that characterization methods for OAWG fields offer high sensitivity (low power requirement) and fast data acquisition. These properties will be needed when pulse shaping is operated at rapid waveform updates [10] and also to capture interesting waveform transients expected with both high (line by line) spectral resolution and very rapid waveform update [11].

A few efforts towards waveform characterization for OAWG have been reported. For example, in [12] spectral phase was measured by observing the phase of the RF beat signal obtained when a line by line shaper was used to select two adjacent comb lines at a time from a 10 GHz frequency comb. In [3] signals from a 20 GHz optical comb were characterized by an X-FROG [13] technique in which the sum frequency signal generated through the interaction of shaped and unshaped fields was spectrally resolved and measured as a function of delay. However, both of these techniques require a series of measurements performed sequentially, which slows measurement time.

In this paper, for the first time to our knowledge, we adapt a technique known as dual-quadrature spectral interferometry [9] for measurement of OAWG waveforms and demonstrate its ability to characterize OAWG fields composed of ~30 spectral lines at 10 GHz line spacing with 1.4 μ s data acquisition time. In conventional implementations of spectral interferometry, reference and signal fields must be separated in time in order to achieve unambiguous phase retrieval. This implies a delay exceeding the temporal aperture of the waveform being measured. Such large delay increases demands on spectral resolution, which is already a significant challenge in OAWG. In fact, from a fundamental perspective, for a periodic waveform with a 100% duty cycle, it is impossible to achieve time separation greater than the temporal aperture of the waveform since delay will also be periodic at the repetition rate. However, in dual quadrature spectral interferometry two orthogonal polarization states are used to simultaneously obtain the in-phase and quadrature components of the interference signal. This allows unambiguous phase retrieval at zero delay setting, which reduces the spectral resolution requirement to approximately the frequency spacing of the comb. Also, since spectral interferometry is a linear technique, it can potentially work at very low signal power.

It is important to recall that spectral interferometry is not self-referencing and requires a well characterized reference field with respect to which the unknown signal field is measured. However, since the reference field may consist of short pulses that are isolated in time, standard techniques such as FROG and SPIDER may be applied to characterize the reference [13, 14]. Once the reference pulse is characterized, a single measurement suffices for each waveform retrieval. Although the dual-quadrature scheme has been used previously to characterize high frequency pulse trains for telecommunication purposes [15], to our knowledge our work is the first to apply it to measure complex OAWG fields, a situation in which the benefits of dual quadrature spectral interferometry become most evident.

2. Mathematical description

In dual-quadrature spectral interferometry, in-phase and quadrature interferograms ($I_1(\omega)$ and $I_2(\omega)$) can be written in terms of the signal and reference power spectra ($|A_s(\omega)|^2$ and $|A_r(\omega)|^2$) and the phase difference between them ($\Delta\psi(\omega)$) as [9]

$$I_1(\omega) = |A_s(\omega)|^2 + |A_r(\omega)|^2 + 2|A_s(\omega)||A_r(\omega)|\cos(\Delta\psi(\omega)) \quad (1)$$

$$I_2(\omega) = |A_s(\omega)|^2 + |A_r(\omega)|^2 + 2|A_s(\omega)||A_r(\omega)|\sin(\Delta\psi(\omega)) \quad (2)$$

The reference spectrum and phase and the two interferograms are known and from the two equations we need to retrieve the signal spectrum and the signal phase. In general the above equations give two solutions for the signal spectrum and phase which are

$$|A_s|^2 = \frac{(I_1 + I_2)}{2} \pm \frac{\sqrt{(I_1 + I_2)^2 - 2(I_1^2 + I_2^2) - 4|A_r|^4 + 4|A_r|^2(I_1 + I_2)}}{2} \quad (3)$$

with the corresponding $\Delta\psi(\omega)$ for each $|A_s(\omega)|^2$ given by

$$\Delta\psi(\omega) = \arg\left(\frac{(I_1(\omega) - |A_s(\omega)|^2 - |A_r(\omega)|^2) + j(I_2(\omega) - |A_s(\omega)|^2 - |A_r(\omega)|^2)}{2|A_s(\omega)||A_r(\omega)|}\right) \quad (4)$$

This however prevents unambiguous retrieval with a single measurement and requires an auxiliary measurement, e.g., of the signal power spectrum. In previous demonstrations a separate measurement of the signal spectrum was in fact carried out [9, 15]. Here we show that with an additional constraint which can be easily implemented in the experiment, Eq. (1) and Eq. (2) are sufficient to unambiguously retrieve both the signal spectrum and the phase information.

Adding Eq. (1) and Eq. (2) we have,

$$|A_s|^2 = \frac{(I_1 + I_2)}{2} - (|A_r|^2 + \sqrt{2}|A_s||A_r|\sin(\Delta\psi + \pi/4)) \leq \frac{(I_1 + I_2)}{2} - (|A_r|^2 - \sqrt{2}|A_s||A_r|) \quad (5)$$

Now if we require that the level of the signal spectrum is less than the reference spectrum everywhere by at least 3dB (i.e. $|A_s(\omega)|^2 \leq |A_r(\omega)|^2 / 2$ for all ω), then $|A_r(\omega)|^2 - \sqrt{2}|A_s(\omega)||A_r(\omega)| \geq 0$, and so from Eq. (5) we have $|A_s(\omega)|^2 \leq \frac{(I_1(\omega) + I_2(\omega))}{2}$. This

forces the negative sign for the signal spectrum in Eq. (3) and thus ensures uniqueness for the spectrum and the corresponding spectral phase. Also, our new constraint is not hard to implement since in most spectral interferometry implementations, the signal and reference are derived from the same source; it is therefore sufficient to ensure that the net gain in the signal arm is less than that in the reference arm by 3dB.

3. Experimental setup

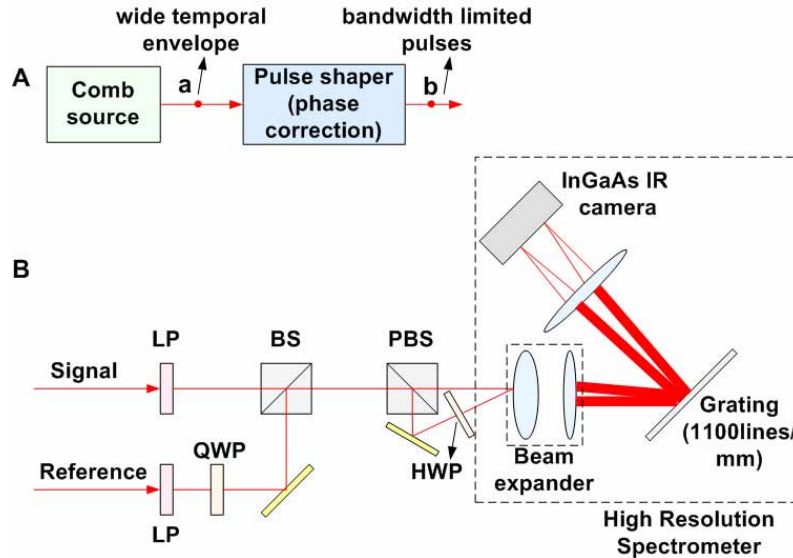


Fig. 1. (a) Schematic showing the generation of bandwidth limited pulses. At point (a) the frequency comb has a wide temporal envelope which is then phase corrected to obtain compressed bandwidth limited pulses at point (b). (b) Experimental setup, LP : linear polarizer, QWP : quarter wave plate, HWP : half wave plate, BS : beam splitter, PBS : polarizing beam splitter.

Figure 1(a) shows the functional representation of the input source used for our experiments. The comb source consists of a CW laser with specified 1 kHz line width at a center wavelength of 1542nm sent to a dual-modulation comb generator, where a low- V_{π} phase modulator is driven at $2 \cdot f_{\text{rep}}$ (20GHz), which defines the overall bandwidth, and a subsequent intensity modulator is driven at f_{rep} (10GHz), which defines the line spacing. At point (a) in the figure, the field is still spread in time, since the phases of different frequency components are not yet corrected. A bandwidth-limited pulse is then obtained at (b) by phase correcting individual frequency components in a line-by-line pulse shaper. Our procedure involves adding one comb line at a time (starting with three) and adjusting the phase of the new frequency component (with step sizes of $\pi/12$) in order to maximize the second harmonic generation signal from an autocorrelator set at zero delay [16]. After phase correction, the intensity autocorrelation is found to be in excellent agreement with that of the pulse simulated assuming flat spectral phase. This gives us confidence that the compressed pulse is corrected close to the zero phase condition. A portion of the compressed pulse is used as the reference for subsequent spectral interferometry experiments.

Figure 1(b) shows the dual quadrature spectral interferometry setup. The signal to be measured is linearly polarized at a 45deg angle while the reference is circularly polarized. These two beams are combined followed by a high resolution spectrometer consisting of a 10X beam expander, an 1100lines/mm grating, and an InGaAs IR CCD camera [Andor, 17].

The pixel dimension of the camera in the dispersed direction is 25 microns, which corresponds to a spectrometer resolution of 3.33 GHz per pixel. This gives a line to line spacing of 3 pixels on the camera (corresponding to the frequency comb spacing of 10 GHz). The spectrometer simultaneously measures the interferograms in both polarizations (corresponding to the in-phase and quadrature terms) by mapping them to different physical locations on the camera. The measured spectrometer crosstalk arising from a single adjacent line three pixels away is ~5% and ~8%, respectively, for the two channels. For each of the polarizations, the 30 lines of the frequency comb spread across 90 pixels of the camera. We retrieve waveform information from a single frame of CCD data with 1.4 μ s integration time, which defines our data acquisition time. In our measurements we have verified good waveform retrieval at an average signal and reference power of 10 μ W and 20 μ W. In this case, since the total energy per measurement is a product of the signal power and the gating time, we are only using around 14 pJ of signal energy per measurement. This corresponds to an average signal energy of less than 0.5 pJ per spectral line. The fast acquisition time significantly reduces sensitivity to environmental fluctuations. For example, at 1.4 μ s integration time optical phase fluctuations associated with the relatively long (up to 50 km, as detailed later) lengths of optical fibers did not appear to degrade our spectral interferometry data.

4. Results

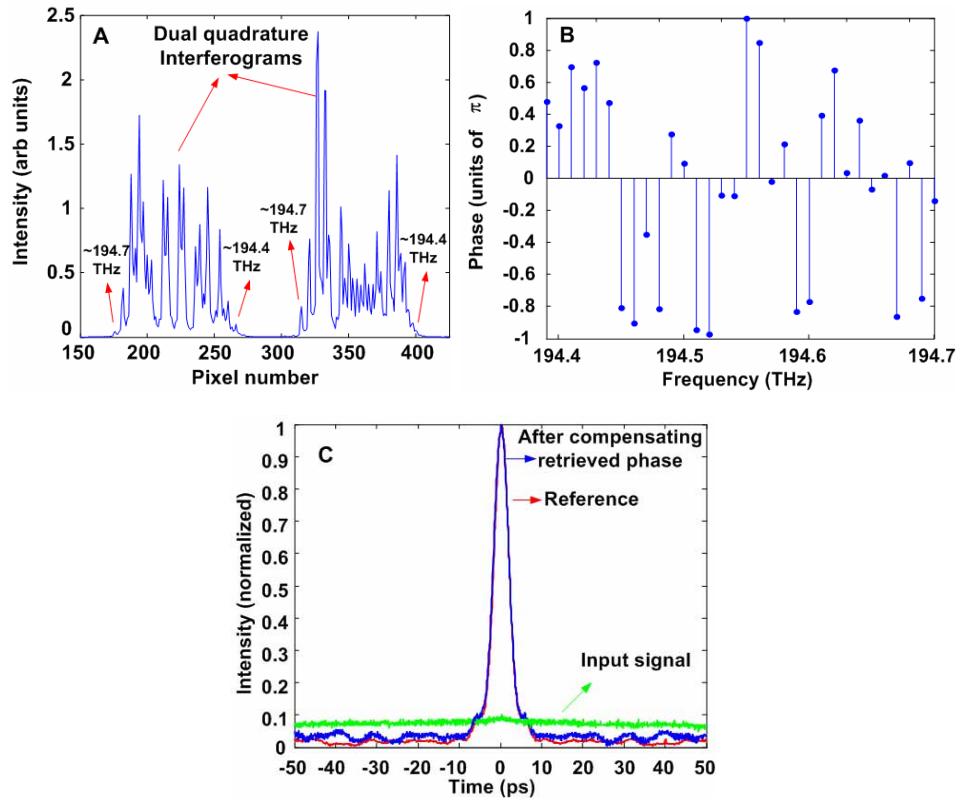


Fig. 2. (a) Raw interferogram data obtained by the camera showing the two quadratures. (b) Retrieved spectral phase. (c) Experimental autocorrelations showing the reference pulse and the signal before and after applying the inverse of the retrieved phase.

In Fig. 2 we describe the results of an experiment that demonstrates the ability to characterize fields spanning the full 100 ps waveform period at 100% duty cycle. As noted before, although a frequency comb is formed after the modulators, in the time domain the envelope is

still spread over most of the 100 ps period. This situation corresponds to strong spectral phase variation. The bandwidth-limited reference pulse formed by compressing the comb (extracted from point (b) in Fig. 1(a)) is then used to measure a signal field corresponding to an uncompressed version of the frequency comb (extracted from point (a) in Fig. 1(a)) through the dual-quadrature spectral interferometry. The inverse of the retrieved phase is applied to the signal field via a second line-by-line shaper (not shown), and the output autocorrelation is measured. If the phase retrieval is good, the autocorrelation should be that of a bandwidth-limited output pulse matching that of the reference pulse. In Fig. 2(a) we show representative raw interferogram data obtained from the camera showing both the channels. Each pixel corresponds to ~ 3.33 GHz, which corresponds to a spacing of 3 pixels between adjacent lines of the frequency comb. Abrupt changes in the intensities of the interferograms indicate the strong phase variation which occurs on a line by line basis. In Fig. 2(b), we have the retrieved spectral phase. We see a strongly modulated phase pattern with abrupt phase jumps. Fig. 2(c) shows the autocorrelations of the input signal field (uncompensated comb), which has a nearly flat envelope and occupies the entire 100ps repetition period, as well as those of compressed reference and signal pulses. The autocorrelations of the reference pulse compressed under the second harmonic optimization method [16] and of the signal pulse compressed under spectral interferometry control are closely matched and correspond to bandwidth-limited pulses ~ 3 ps in duration. The slight increase in the wings of compressed pulse autocorrelation compared to those of the reference pulse can be attributed to small errors in the spectral interferometry measurement.

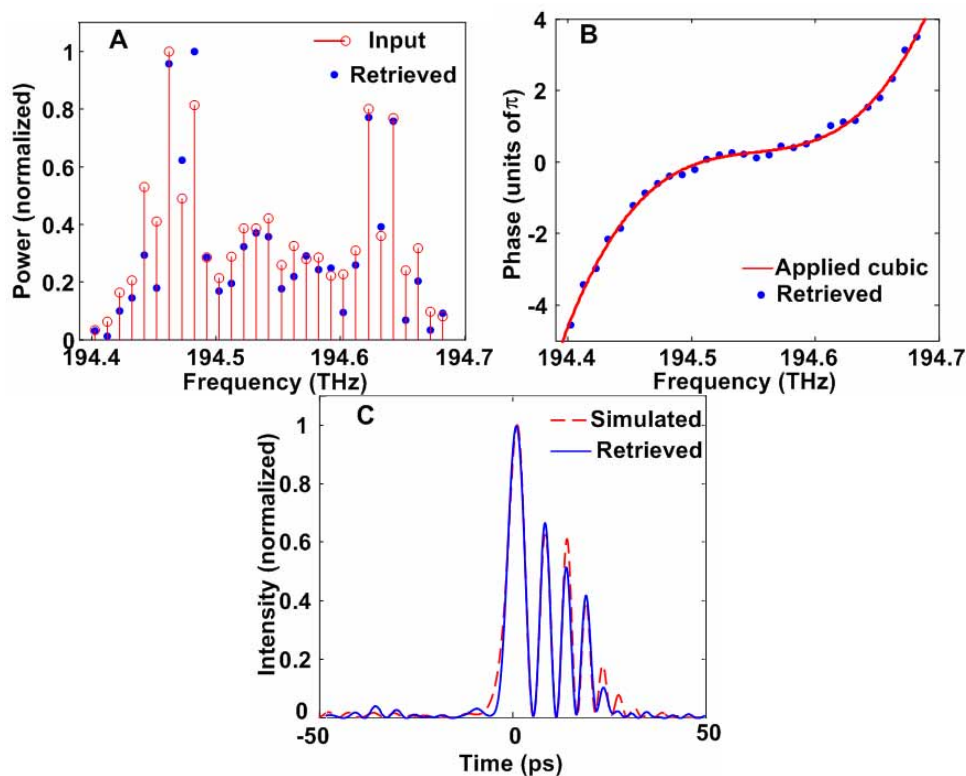


Fig. 3. (a) Input and retrieved spectra. (b) Applied cubic phase and the retrieved spectral phase. (c) Time domain intensities generated using the retrieved spectrum and phase (retrieved) and the input spectrum and applied phase (simulated).

Figure 3 demonstrates the use of spectral interferometry for retrieval of the power spectrum and phase of a signal field to which known user defined spectral phase was applied.

Here the compressed pulse (at point (b) in Fig. 1(a)) is split to yield identical reference and signal pulses. Cubic spectral phase was then applied using a second line by line shaper operating only on the signal field. In Fig. 3(a), the input spectrum (measured independently on an OSA) and the retrieved spectra are plotted. Fig. 3(b) shows both the applied phase (i.e., the phase programmed onto the pulse shaper) and the retrieved phase. The retrieved phase is in good agreement with the applied cubic phase; the difference has a standard deviation of 0.11π radians. Simulations show that the difference between the applied spectrum and phase and the retrieved spectrum and phase arise mainly due to the crosstalk in the spectrometer. By further reducing the crosstalk, improvement should be possible. In Fig. 3(c), we show a comparison of calculated time domain intensity profiles obtained using the input power spectra (measured separately) and the applied spectral phase or that retrieved through spectral interferometry. The close agreement indicates that the phase measurement through spectral interferometry is sufficiently accurate to yield a meaningful prediction of field profile in the time domain.

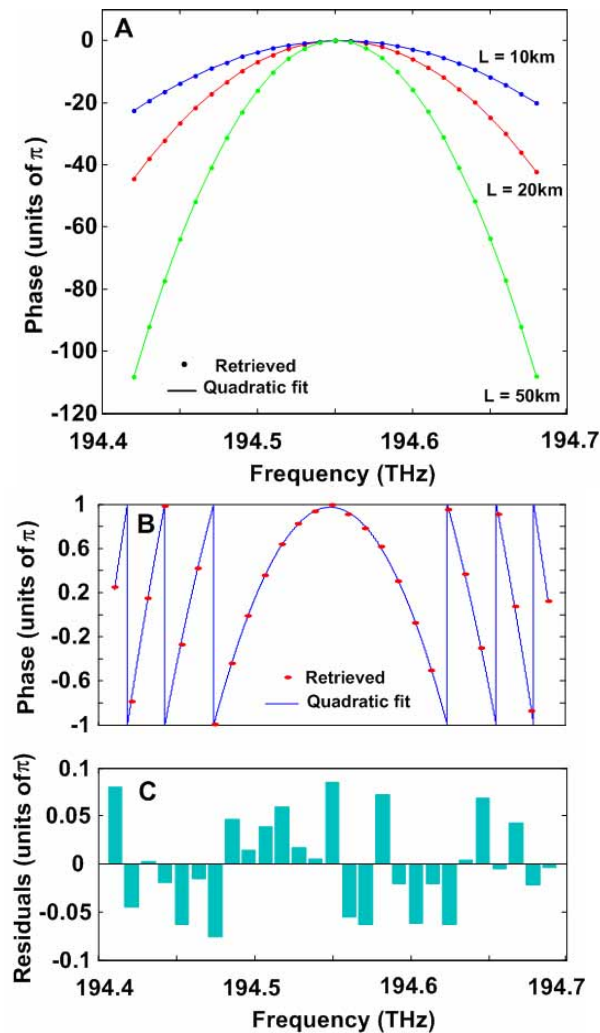


Fig. 4. (a) Retrieved spectral phases after propagation over 10km, 20km and 50km of optical fiber. The solid lines represent the quadratic fit. (b) The retrieved phase and the quadratic fit, shown without the unwrapping and (c) the corresponding residuals for the 10 km fiber.

The relative immunity to environmental fluctuations provided by the fast measurement time allows us to make coherent waveform measurements over long lengths of optical fiber. This may provide a method to measure frequency dependent phase fluctuations relevant to transfer of precise timing information transfer over optical fibers [18, 19]. Fig. 4(a) shows the measured spectral phase of the signal field after propagation through 10km, 20km and 50km of standard single mode optical fiber. The quadratic fit to the data is also shown. The standard deviation of the error between the measured phases and the quadratic fit is 0.05π , 0.04π , 0.07π respectively corresponding to 10km, 20km and 50km. The amount of cubic phase present in these cases is small. As additional verification, from the retrieved phase and the knowledge of the length of the each fiber spool, the dispersion coefficients were calculated to be 16.4ps/nm km, 16.4ps/nm km and 16.2ps/nm km. These independent estimates are all very close and are consistent with the known dispersion of standard single mode fiber.

The total dispersion corresponding to the three different fiber spools turn out to be ~400ps, 800ps and 2000ps, respectively, which are all significantly higher than the pulse period of 100ps. This means that the net change in phase over the entire bandwidth is significantly higher than 2π . Therefore, the underlying quadratic phase moves over many 2π ranges over the frequency range, with the variation becoming more rapid as we move away from the center. Our measurement samples this nominal quadratic function periodically at 10GHz intervals. To indicate this, Fig. 4(b) shows the retrieved phase and the corresponding quadratic fit for the case of 10km fiber length, but in this case without the unwrapping. As expected, the retrieved phase lies close to the wrapped quadratic fit. We notice that as we move away from the center frequency in Fig. 4(b), the measurement points sample the quadratic phase only one or two times per 2π variation. We might expect this to raise questions about the adequacy of the sampling frequency and whether a subset of the data from the above figure (say farther away from the center frequency) is sufficient to unambiguously provide the underlying quadratic phase.

To address this issue, we would like to point out that the choice of starting the unwrapping with smallest variation near the center was arbitrary which would make the points away from the center seem to have greater variation from point to point. We could have started the unwrapping near any point in which case, the phase variation would be minimum near that point. The underlying reason here is that the different quadratic fits that are obtained while we vary the choice of the data point to start unwrapping differ only by a linear phase (because shifting the center frequency for a function which is quadratic in frequency gives a term linear in frequency). Hence, even a subset of the data from the above figure uniquely determines the underlying quadratic phase and by subtracting different amounts of linear phase, can be made to look symmetric(having minimum variation) around any point. This point is further clarified in Fig. 4(c) where we plot the residuals (difference between the quadratic fit and retrieved phase) for each data point. The magnitude of the residuals don't show any pronounced character while moving away from the center frequency and the variations are of the same order indicating the similarity of each retrieved data point. Similar behavior is observed in the residuals of the 20km and 50km fiber measurements.

Reconstructing the underlying quadratic phase from the retrieved phase truly becomes ambiguous when the phase becomes large enough that the derivative (which is a linear function) has a phase difference greater than 2π between two data points. This happens at around 75km of optical fiber for the case when we sample at 10GHz. This means that when we reconstruct the quadratic phase for a retrieval with 75km of fiber, it would look like having no optical fiber. In time domain this would correspond to the situation where a bandwidth limited pulse train after linear dispersive propagation over this distance would reform and look identical to when it started (neglecting transmission losses and higher order spectral phases). If it becomes necessary to unambiguously measure the dispersion corresponding to >75km lengths of standard fiber, then the spectral resolution needs to be increased appropriately.

5. Summary and future work

In summary, we have demonstrated the use of dual-quadrature spectral interferometry for measurement of OAWG waveforms composed of ~30 spectral lines at 10 GHz line spacing with 1.4 μ s data acquisition time. We have also demonstrated that our technique enables direct, coherent measurements of spectral phase even after propagation over 50km of optical fiber. A particular advantage with respect to characterization of OAWG signals is that spectral resolution requirements are reduced to approximately the frequency spacing of the comb. Our experiments are currently limited by the total bandwidth available from the comb source but can accommodate increased bandwidth by using more pixels on the IR CCD camera. In the future it should become possible to use our technique to measure waveform transients that will occur when OAWG is coupled with very fast waveform switching.

Acknowledgments

This work is supported by the DARPA/ARO under grant W911NF-07-1-0625 and by the NSF under grant ECCS-0601692. We would like to thank Chen-Bin Huang and Fahmida Ferdous for help with the optical frequency comb source.